JOURNAL OF MATERIALS SCIENCE 20 (1985) 3213 – 3218

Effect of Al_2O_3 particles on the growth kinetics of molybdenum grains in liquid nickel

SUK-JOONG L. KANG, DUK N. YOON
Department of Materials Science and Engineering, Korea Advanced Institute of Science and Technology, P.O. Box 131 Chongryang, Seoul 131, Korea

Grain growth inhibition by inert third phase particles during liquid phase sintering has been investigated in Mo–Ni alloys containing Al_2O_3 particles sintered at 1460° C. The grain growth is inhibited slightly by the Al_2O_3 particles, and this result is explained in terms of the shielding of material precipitation at the contact area and of the suppression of material precipitation around the contact area, which is determined by the dihedral angle between the molybdenum grain and the Al_2O_3 particle. The result is compared to those obtained earlier with specimens containing highly soluble third phase particles.

1. Introduction

Grain growth inhibition by a small amount of second phase particles in two-phase systems is explained essentially by the well-known Zener effect [1]. The effect of a third solid phase on grain growth in three-phase systems (solid A–solid C–liquid B), however, is not well understood. Experimental results [2–5] have previously shown that the grain growth of solid A was strongly inhibited by the presence of a small amount of solid C in liquid matrix B. White [3] attributed this grain growth inhibition effect to the changes in the curvature of solid/liquid interfaces of the growing grains of solid A in contact with the grains of solid C. Warren [5] explained the inhibition effect as due to the lower mobility of contiguous grain boundaries between different phases. The growth behaviour of solid A, however, is expected to be also influenced by the solubilities of the components of solid C in liquid B and thus the change of liquid and grain compositions. In the previous experimental systems [2–5], coarsening of solid C occurred simultaneously with that of solid A.

In the present investigation, the grain growth behaviour in three-phase systems containing essentially inert third phase particles has been studied. Mo–Ni alloys with and without Al_2O_3 particles have been prepared in order to examine the effect of small amounts of these inert particles on the rate of molybdenum grain growth. The solubility and the growth rate of Al_2O_3 in liquid nickel are both negligible compared to those of molybdenum in liquid nickel [6].

2. Experimental procedure

The experimental procedure was similar to those described in previous studies [7, 8]. Four different Mo–Ni specimens with or without Al_2O_3 particles were prepared. Binary Mo–Ni (96Mo–4Ni and 95Mo–5Ni wt %) alloys were prepared from molybdenum powder of 7 μm (FSSS) and nickel powder of 1.7 μm. Specimens containing Al_2O_3 (95Mo–4Ni–1Al_2O_3) and 94.4Mo–5Ni–0.6Al_2O_3) were prepared by adding Al_2O_3 particles of 30 μm in average diameter to molybdenum and nickel powders. The dry mixed powders were pressed under 100 MPa into cylindrical compacts 10 mm diameter and approximately 5 mm high. The compacts were presintered at 900° C for 4 h and sintered at 1460° C for various times in a tube furnace under flowing hydrogen. The heating and cooling rate was approximately 30 K min^{-1}.

0022–2461/85 $03.00 + .12

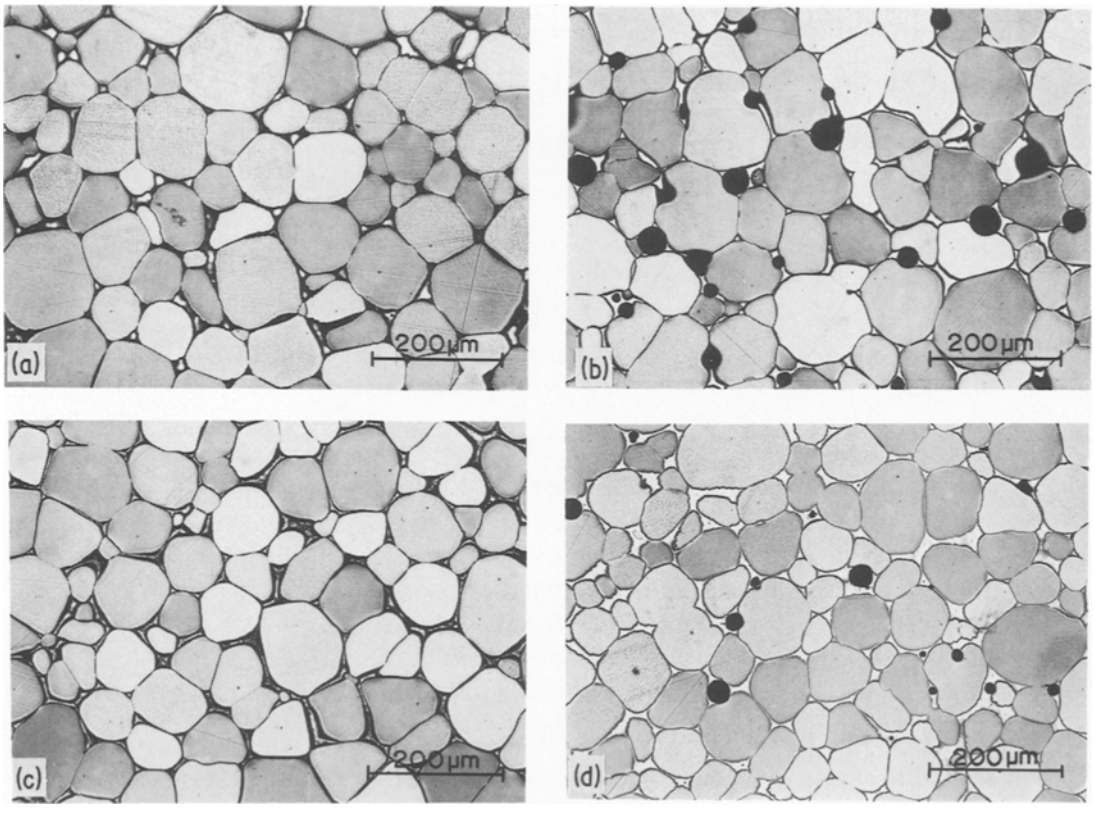

Figure 1 Microstructures of (a) 96Mo–4Ni, (b) 95Mo–4Ni–1Al_2O_3, (c) 95Mo–5Ni, and (d) 94.4Mo–5Ni–0.6Al_2O_3 specimens sintered at 1460° C for 8 h.

The average cross-sectional area of the grains, $\bar{A}$, was obtained from the grain volume fraction and grain frequency per unit cross-sectional area [8, 9]. The average cross-sectional radius, $\bar{r}$, was calculated from the relation $\bar{r} = (\bar{A}/\pi)^{1/2}$*. For each specimen, the grains within the area of 15 500 to 31 000 μm^2 (about 300 to 700 grains) on two or four photomicrographs taken at different areas were measured.

3. Experimental results

Microstructures of the sintered specimens are shown in Fig. 1. Figs. 1a and c show typical liquid phase sintered structure of Mo–Ni specimens. The microstructures of the specimens containing Al_2O_3 shown in Figs. 1b and d reveal that the molybdenum grains in contact with Al_2O_3 particles have grown around Al_2O_3 particles with a concave curvature at the contact areas.

The average measured volume fractions of the phases and their standard deviation are shown in Table I. The specimens with 5 and 4 wt % Ni have, on the average, 9.6 and 7.5 vol % liquid phase. The liquid contents calculated from the Mo–Ni phase diagram [10] are approximately

TABLE I Measured average volume fraction of phases

Specimen	Phase (vol %)		
	Solid	Liquid	Al_2O_3
96Mo–4Ni	92.7 ± 0.7	7.3 ± 0.7	
95Mo–4Ni–1Al_2O_3	89.3 ± 1.6	7.7 ± 1.4	3.0 ± 0.5
95Mo–5Ni	90.8 ± 1.8	9.2 ± 1.8	
94.4Mo–5Ni–0.6Al_2O_3	87.7 ± 1.0	10.0 ± 0.9	2.3 ± 0.7

*The actual average grain radius can be obtained by multiplying a proportionality constant to $\bar{r}$ with a known size distribution [9].

TABLE II Measured average cross-sectional grain radius (μm)*

Time (h)	96Mo–4Ni $\bar{r}$	95Mo–4Ni–1Al_2O_3 $\bar{r}(\bar{r}_{ex})^{\dagger}$	95Mo–5Ni $\bar{r}$	94.4Mo–5Ni–0.6Al_2O_3 $\bar{r}(\bar{r}_{ex})$
2	–	25.6 (25.7)	25.5	25.1 (25.2)
4.2	33.7	32.6 (32.8)	32.3	31.4 (31.5)
8	42.2	40.7 (41.2)	41.2	39.5 (39.8)
16	55.2	52.6 (53.1)	52.4	50.8 (51.2)

*This grain radius is not a conventional average grain radius. The average cross-sectional grain radius ($\bar{r}$) is obtained from the average cross-sectional area ($\bar{A}$) using the relation $\bar{r} = (\bar{A}/\pi)^{1/2}$.
†$\bar{r}$ and $\bar{r}_{ex}$ are average and extended average grain radii, respectively. See text for the implications of these different radii.

9% and 7%, respectively, for specimens with 5% and 4% Ni, in good agreement with the measured values.

Table II summarizes the increase of average cross-sectional grain radius, $\bar{r}$, with sintering time. The average grain radius of the specimens containing Al_2O_3 was determined in two different ways. The average radii, $\bar{r}$, in the table (without parentheses) were obtained from the average cross-sectional areas of the molybdenum grains. These values represent the average cross-sectional molybdenum grain radius when the grains are assumed to be spherical. In determining the average radii in parentheses (extended average radii, $\bar{r}_{ex}$), the volume fraction of the grains was taken to be different from that for the average grain radii, $\bar{r}$. For grains in contact with Al_2O_3 particles, the shape of the grains was assumed to be roundish, as in Mo–Ni specimens, and a part of the Al_2O_3 particles and of liquid was included in calculating the volume of the grains, as schematically shown in Fig. 2. This measurement would allow the elimination of the local effect of Al_2O_3 particles on grain growth.

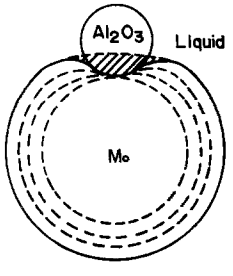

Figure 2 Schematic illustration of two different ways for the determination of molybdenum grain size in contact with Al_2O_3 particle (a) without and (b) with taking into account the hatched area. The dashed lines illustrate schematically the growth behaviour of the molybdenum grain under the assumption that no material change occurs at the contact area.

Fig. 3 shows the relationship between the cube of the average cross-sectional grain radius, $\bar{r}^3$, and the sintering time, t. A linear relationship between $\bar{r}^3$ and t is well maintained except at 16 h. This discrepancy probably arises from the decrease of the liquid content by evaporation during prolonged sintering. For specimens sintered for 16 h, the amount of liquid was found to be approximately 1% less than the average values shown in Table I. The linear relation between $\bar{r}^3$ and t agrees with the previous experimental results on similar two phase alloys with the low liquid contents [8, 11, 12].

4. Discussion

In the previous studies on liquid phase sintered Mo–Ni–Al_2O_3 alloys, the growth behaviour of molybdenum grains around Al_2O_3 particles was determined by etch boundaries formed by a cyclic sintering treatment [7, 13]. Fig. 4 shows a typical microstructure of a cyclically sintered 94.4Mo–5Ni–0.6Al_2O_3 alloy. The inhibited growth of large molybdenum grains in contact with Al_2O_3 particles is revealed by the etch boundaries within the grains, which are schematically shown in Fig. 2 by the dashed lines. The etch boundaries converge at the contact area indicating that no material had precipitated in this area and that material precipitation had been suppressed at the grain surfaces adjacent to the Mo–Al_2O_3 junction during grain growth.

The absence of material precipitation at the contact area appears to arise from the shielding of material flux by Al_2O_3 particles under the influence of the compressive pressure due to liquid meniscus at the specimen surface [7, 14]. Since material transport to the contact area is limited by the small cross-section of the liquid film at that area [7], material change at the contact area will be small. The contact boundaries

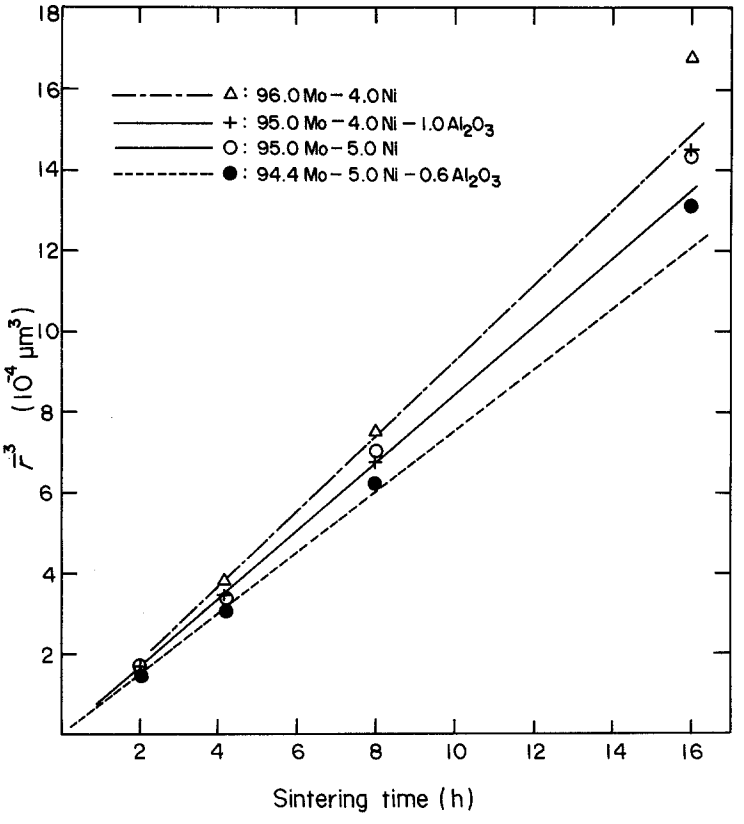

Figure 3 Observed increase of the average cross-sectional grain radius with sintering time.

of growing molybdenum grains can thus appear to be immobile relative to Al_2O_3 particles in contact.

The suppression of material precipitation near the contact area, on the other hand, is probably determined by the dihedral angle† between the molybdenum grain and the Al_2O_3 particle, since any appreciable deviation from the dihedral angle condition at the Mo/Al_2O_3/liquid junction, brought about by material deposition at the surrounding region, may require diffusions by molybdenum in liquid over a distance of a few atomic units before the surface tension condition at the junction can be restored. As the dihedral angle in this system is 0° [7], the precipitation of material at the molybdenum/liquid interface near the contact area must be inhibited, if the dihedral angle of 0° is to be maintained, resulting in a converging growth behaviour of molybdenum grains at the contact area.

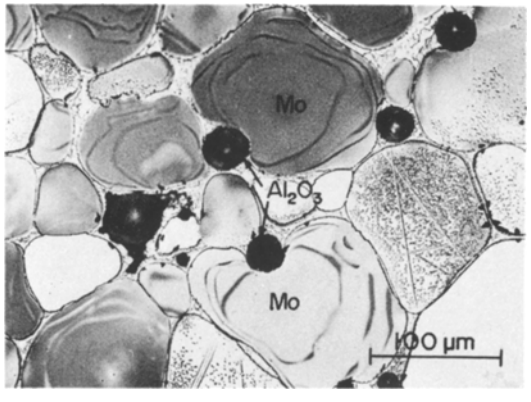

Figure 4 Typical etch boundaries within growing molybdenum grains in contact with Al_2O_3 particles in a 94.4Mo–5Ni–0.6Al_2O_3 alloy cyclically sintered at 1460° C with four holding times (1 + 1 + 1 + 1 h).

Therefore, the effective amount of growth inhibition due to an Al_2O_3 particle is reflected as the difference between the volume of a growing grain which is in contact with other grains or immersed in liquid matrix and the volume of a growing grain which is in contact with the Al_2O_3 particle. This volume difference is schematically shown by the hatched area in Fig. 2.

The difference between the average grain

†The dihedral angle between two phases is not a conventional one, since only the force component perpendicular to the radial direction of the spherical third phase particle is satisfied [7].

TABLE III Observed growth rate constants of three-phase alloys in comparison with those of two-phase alloys with equal amount of liquid (k)*

White [3], $CaO–MgO–Fe_2O_3$†		Stephenson and White [4], $CaO–MgO–Al_2O_3–SiO_2$†		Warren [5], NbC–VC–Co†		This work, Mo–Ni–Al_2O_3	
$CaO(MgO, Fe_2O_3)$ + 3 vol % MgO (CaO, Fe_2O_3)	$\sim 0.7k$	CaO(Mg, Al, Si, O) + 9 vol % MgO (Ca, Al, Si, O)	$\sim 0.6k$	(Nb, V)C + trace (V, Nb)C	$< k$ ($\sim 0.7k$)	Mo(Ni) + 3 vol % Al_2O_3	$\sim 0.9k$
$MgO(CaO, Fe_2O_3)$ + 3 vol % CaO (MgO, Fe_2O_3)	$\sim 0.6k$			(V, Nb)C + trace (Nb, V)C	$\sim 10^{-3}k$		

*The rate constant, k, was obtained using the relation, $r^3 = kt$, which was found to be maintained for the studied range, where r and t are average grain radius and sintering time, respectively.
†The rate constant was calculated from the reported grain radii for certain sintering times.

radius, $\bar{r}$, and the extended average grain radius, $\bar{r}_{ex}$, of specimens containing Al_2O_3 particles in Table II can thus be interpreted to be a result of grain growth inhibition due to material shielding and a dihedral angle of 0°. The relative volume difference obtained from the third power of the average and the extended average radii is less than 4%, implying that this inhibition effect is very small. It appears, however, that the inhibition effect increases with sintering time. This result may arise from the increase in the volume of Al_2O_3 particles and of liquid with grain growth, both increases of which are included in the volume fraction of grains for the calculation of $\bar{r}_{ex}$. Comparing the average radii of specimens containing Al_2O_3 particles with the extended average radii in Table II, these inhibition effects are shown to be higher with larger amounts of Al_2O_3 particles.

The overall grain growth in these alloys is only slightly inhibited by a small amount of Al_2O_3 particles. Table III summarizes the observed growth rate constants of three-phase alloys studied in this and in previous investigations [3–5] in comparison with those of two-phase alloys. The liquid contents in two-phase and in three-phase alloys are approximately equal in each system investigated. From this table, it is evident that the effect of the third phase on grain growth rate varies greatly depending on the alloy system under investigation and also on the kind of third phase for the system concerned. It is noteworthy that essentially inert Al_2O_3 particles have a much smaller effect on the grain growth rate than other third phases soluble in liquid. These results suggest the existence of a strong effect on grain growth of the solubilities of the components of the third phase. With the presence of third phase particles soluble in liquid and in growing solid grains, and themselves coarsening, the composition of growing grains and liquid matrix become different from those in two-phase alloys. The growth kinetics of the three-phase alloys can consequently deviate from that of the two-phase alloys. Furthermore, when two grains of different phases are in close contact with each other, the difference in solubilities of each component in liquid may affect each other's growth rate.

5. Conclusion

In this study, the effect of inert third phase particles on grain growth in liquid matrix could be determined by comparing the grain size and the amount of phases in the Mo–Ni specimens with and without Al_2O_3 particles. The grain growth inhibition was found to be not as large as previously expected, and limited to the vicinity of the region in contact with Al_2O_3 particles. When the third phase particles are soluble in liquid matrix, as in previous investigations, the solubilities of the components of the third phase may affect the grain growth rate.

Acknowledgements

The authors wish to express their gratitude to Professor G. Petzow for his support and to W. A. Kaysser for helpful discussions. This work was partially done under a joint research programme between Deutsche Forshungsgemeinschaft (DFG) and Korea Science and Engineering Foundation (KOSEF). One of the authors (S-JLK) is grateful to KOSEF and DFG for financial support.

References

1. C. S. SMITH, *Trans. AIME* **175** (1948) 15.
2. O. K. RIEGGER, G. I. MADDEN and L. H. VAN VLACK, *ibid.* **227** (1963) 971.
3. J. WHITE, in "Ceramic Microstructures", edited by R. M. Fulrath and J. A. Pask (John Wiley, New York, 1968) p. 728.
4. I. M. STEPHENSON and J. WHITE, *Trans. Brit. Ceram. Soc.* **66** (1967) 443.
5. R. WARREN, *Planseeberichte für Pulvermetallurgie* **20** (1972) 299.
6. J. A. DROMSKY, F. V. LENEL and G. S. ANSELL, *Metall. Trans. AIME* **224** (1962) 236.
7. S. -J. L. KANG, W. A. KAYSSER, G. PETZOW and D. N. YOON, *Acta Metall.* **33** (1985) in press.
8. S. S. KANG and D. N. YOON, *Metall. Trans. A.* **13A** (1982) 1405.
9. S. S. KANG, S. T. AHN and D. N. YOON, *Metallography* **14** (1981) 263.
10. S. -J. L. KANG, Y. D. SONG, W. A. KAYSSER and H. HOFMANN, *Z. Metallkde* **75** (1984) 82.
11. K. W. LAY, *J. Amer. Ceram. Soc.* **51** (1968) 373.
12. R. WARREN, *J. Mater. Sci.* **7** (1972) 1434.
13. S. -J. L. KANG, W. A. KAYSSER, G. PETZOW and D. N. YOON, in "Sintered Metal–Ceramic Composites", edited by G. S. Upadhyaya (Elsevier, Amsterdam, 1984) p. 293.
14. H. H. PARK, MS Thesis, Korea Advanced Institute of Science and Technology, Seoul (1982).

Received 17 September
and accepted 15 October 1984